

Received 14 May 2024, accepted 30 May 2024, date of publication 5 June 2024, date of current version 9 July 2024.

Digital Object Identifier 10.1109/ACCESS.2024.3409911

RESEARCH ARTICLE

The Design and Analysis of a Lunar Navigation SmallSat for Southern Hemisphere Moon Navigation

XIAO CHEN^{1,2}, YONG ZHENG¹, LAN DU¹, AND ZHONGKAI ZHANG¹

¹College of Geospatial Information, Information Engineering University, Zhengzhou, Henan 450000, China

²Xi'an Satellite Control Center, Xi'an, Shaanxi 710000, China

Corresponding author: Zhongkai Zhang (zhongkai@ashn.org.cn)


This work was supported in part by the National Natural Science Foundation of China under Grant 42304044; and in part by the Natural Science Foundation of Henan Province, China, under Grant 222300420385.

ABSTRACT Being Earth's only natural satellite, the moon is crucial for human space exploration and serves as a vital base for additional deep space endeavors. Cislunar space represents an extensive domain for expanding human habitation beyond terrestrial land and oceans. The pursuit, building, and advancement of cislunar space have escalated the need for cislunar navigational capabilities. Currently, GNSS navigation technology has been well-established for Earth and near-Earth regions and is now being extended to encompass the cislunar realm. Concurrently, the progress in small satellite technology presents fresh opportunities for the rapid and effective implementation of small satellite navigation networks. Addressing cislunar navigation needs, this document suggests creating a navigation system in small space using BDS (BeiDou Navigation Satellite System) time-transfer technology on a compact satellite platform in earth-moon libration point orbits. A variety of orbital paths, such as DRO (Distant Retrograde Orbit) and NRHO (Near Rectilinear Halo Orbit), are employed to form a navigational constellation under the framework of a small satellite platform operating in earth-moon libration point orbits; BDS timing is utilized to compensate for limited payload capacity on small satellites as well as limitations in star clock accuracy. This paper presents the design architecture analysis of such a cislunar space small-satellite navigation system employing BDS time-transfer technology while systematically studying various multi-orbital characteristics adopted by this system along with its corresponding navigational features. Furthermore, observability analysis is conducted on these navigational constellations while evaluating their performance through relevant accuracy indicators across several constellation design scenarios. This paper confirms the practicality and initial efficacy of the cislunar space small satellite navigation system, employing BDS for time-transfer, serving as an essential guide for BDS and GNSS in providing navigational services in cislunar space. An innovative idea and approach for navigating lunar space and the southern hemisphere's moon is suggested.

INDEX TERMS Navigation, LNSS, BDS, time-transfer, DRO, NRHO.

I. INTRODUCTION

Being the closest natural celestial body to Earth, the moon represents humanity's initial foray into exploring the universe. Decades after the Apollo program, both the United States and Russia have initiated plans for lunar return missions. Correspondingly, China, Europe, Japan, and other

The associate editor coordinating the review of this manuscript and approving it for publication was Gerardo Di Martino .

countries have also implemented lunar exploration programs while China has proposed establishing a permanent International Lunar Research Station (ILRS) [1], [2], [3]. China will launch the Chang'e-6 [4], [5], [6] and Chang'e-7 [7], [8], [9], [10] missions to explore the moon. Inevitably, there will be an influx of probes and human activities in both lunar and cislunar space in the future. Establishing services for positioning, navigation, and timing (PNT) [11], [12], [13], which encompass the moon and its adjacent areas, is vital for

the successful execution of both manned and robotic lunar exploration missions. The GNSS provides accurate PNT services on Earth’s surface and in near-Earth space [14], [15], [16]. Furthermore, GNSS satellite clocks can be continuously calibrated through ground-based segments to achieve high accuracy necessary for navigation purposes.

Compared with traditional GNSS systems though limited by certain factors unique to SmallSat platforms used in cis-lunar navigation constellations such as [17], [18], and [19]: a) small size constraining onboard capacity including onboard clocks; b) lower stability of onboard clocks due to cost limitations associated with SmallSat satellites; c) reduced ability of Earth control stations to monitor lunar satellites necessitating less frequent orbit maintenance and clock correction we propose employing high-precision BDS time transfer techniques on low precision SmallSats to enhance their clock accuracy thereby improving overall navigation accuracy within Lunar constellations.

The selection of an appropriate orbit for the construction of a Lunar Navigation SmallSat System (LNSS) in the Earth-Moon space is a crucial step [20], [21], [22], [23]. This article explores the utilization of ELFO (Elliptical Lunar Frozen Orbit), NRHO, and DRO orbits to establish the LNSS. Firstly, these three orbit types exhibit superior stability compared to other libration point orbits, minimizing the need for extensive orbital maintenance maneuvers and reducing reliance on ground support from Earth. The ELFO orbit offers enhanced stability and proximity to the Moon, enabling robust navigation signals. However, it may experience prolonged periods of invisibility with BDS due to onboard clock deviation correction requirements. In contrast, both DRO and NRHO orbits lack significant shielding against BDS interference; nevertheless, DRO orbits can provide continuous coverage across mid-to-low latitude regions of the Moon while NRHO orbits enhance coverage continuity over lunar polar areas.

The primary objective of establishing the LNSS in this study is to minimize the number of satellites required for constructing a satellite navigation system specifically designed for the lunar South Pole region. Previous research has demonstrated that deploying a constellation comprising 24 ELFO satellites across 2 or 3 orbital planes can effectively establish a satellite navigation network covering the entire lunar surface. However, considering the substantial quantity of these 24 satellites, it is more practical to develop a regional satellite navigation constellation that aligns with the scientific objectives of ongoing lunar exploration projects, focusing on addressing current research priorities in the Moon’s South Pole region. Subsequently, by increasing the number of LNSS satellites deployed, we can achieve full coverage for an all-encompassing satellite navigation system catering to lunar missions.

This article aims to enhance the navigation accuracy of the LNSS by utilizing the BeiDou Navigation Satellite System (BDS) for time transfer, based on a SmallSat platform and

Earth-Moon libration point orbits. The LNSS is constructed using multiple small satellite platforms deployed in different Earth-Moon libration point orbits such as DRO, NRHO, etc., with timing synchronization achieved through BDS to compensate for limited payload capacity and onboard clock accuracy of small satellites. 1) Through examining the visibility of satellites in different LNSS and BDS trajectories, we determined the ratio of visible time between SmallSats and several BDS satellites, including measurements such as the Maximum Continuous Invisible (MCI) duration and the longest invisibility period. 2) By transferring timing, we aim to synchronize the onboard clocks of SmallSat satellites with the same level of time accuracy as that provided by BDS. 3) Furthermore, the research examines how LNSS navigates across moon surfaces and low lunar orbit (LLO) satellites, focusing on their navigational precision.

II. METHODOLOGY

This study aims to utilize BDS time transfer for timing by building a Lunar Navigation SmallSat System to provide navigation for users on the lunar surface and in near-lunar orbit (see Figure 1). The BDS constellation is simulated to provide a time reference, and then the LNSS constellation is constructed. Each satellite in the LNSS is equipped with a BDS receiver that points towards Earth to receive and demodulate the BDS signal, which enhances the accuracy of the low-precision satellite clock in LNSS and improves its navigation precision. This study verifies the navigational performance of LNSS in both the lunar surface and near-moon orbit (LLO) constellations by receiving navigation signals transmitted by LNSS. It also confirms the feasibility of enhancing the navigation accuracy of LNSS through BDS timing. The simulation experiment starts on January 1, 2026, at 00:00:00.000 UTC and continues for 30 days. Further details will be provided later in this paper, and the numbers in brackets in Figure 1 correspond to the equations in this paper.

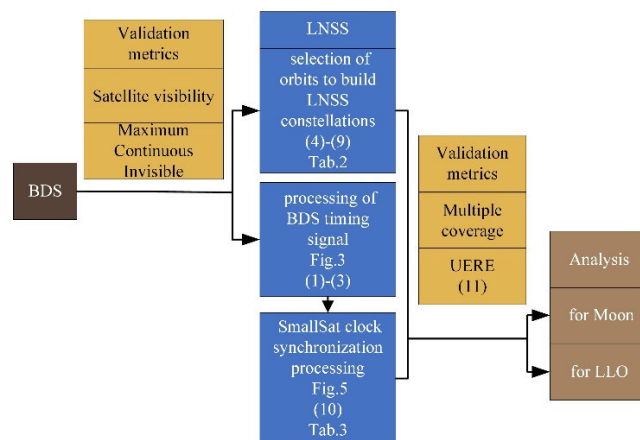


FIGURE 1. A framework of the LNSS proposed system.

A. BDS CONSTELLATION AND TIME TRANSFER FROM BDS

1) BDS CONSTELLATION

To investigate the feasibility of time transfer from BDS to LNSS, we designed a simulated BDS constellation comprising 30 satellites, including 24 MEOs, 3 IGSOs, and 3 GEOs. The BDS satellite orbit in this study was constructed by importing the TLE (Two Line Element) file for establishing the BDS constellation. Utilizing general perturbation theory, the North American Aerospace Defense Command (NORAD) generated a set of elements to predict the position and velocity of Earth’s spacecraft. The TLE published by NORAD was employed to determine the space target’s position. By referencing [24] and querying the NORADID number of BDS-3 satellite, we downloaded the TLE file for BDS-3 from reference [25]. When conducting visibility analysis between Cislunar constellation satellites without considering antenna orientation effects on signal reception, geometric visibility is considered as an indicator for connectivity between LNSS and BDS satellites – implying that LNSS can receive navigation signals transmitted by BDS satellites. In subsequent research endeavors, further analysis will be conducted to establish an accurate spatial transmission attenuation model for signal propagation and assess how satellite antenna directionality influences navigation signal reception.

2) TIME TRANSFER FROM BDS

The selection of an onboard clock is crucial for the navigation satellite system, as its timing stability directly impacts the precision of ranging provided to lunar users. Among various options, we illustrate the use of a commercial Chip Scale Atomic Clock (CSAC) specifically developed for space applications due to its radiation tolerance and compact size, weight, and power (SWaP). By incorporating a BDS antenna on the LNSS satellite, we receive and demodulate BDS signals to obtain time information. This BDS time is then utilized to synchronize the low-precision space-borne clock in order to enhance its accuracy and consequently improve the navigation precision of LNSS. The alternative timing frequencies of BDS are B3I and B1I [26]. The bandwidth of the B3I signal, centered around its carrier frequency, is 20.46 MHz, whereas the bandwidth of the B1I signal, centered at its respective carrier frequency, measures 4.092 MHz. Due to its wider signal bandwidth compared to that of B1I, we select B3I as the primary timing signal, utilizing a carrier frequency of 1561.098 MHz.

TABLE 1. The BDS Service.

Service Types		Signal(s)/ Band(s)	Broadcast Satellites
Worldwide	Positioning, Navigation and Timing (RNSS)	B1I, B3I	3GEO+3IGSO+MEO
		B1C, B2a, B2b	3IGSO+24MEO

We have devised the architecture of LNSS, which leverages the conventional BDS system to deliver precise timing correction for onboard clocks. The functionality of LNSS’s onboard clock is limited, resulting in lower time accuracy. However, by frequently adjusting them through ground stations, BDS onboard atomic clocks achieve high accuracy levels. As illustrated in Figure 1, intermittent utilization of available BDS signals mitigates the necessity for highly accurate onboard clocks and extensive ground monitoring infrastructure. By receiving BDS time updates to synchronize with the relatively less accurate clock of LNSS within an acceptable error range, we meet the precision requirements for Earth-Moon space navigation, specifically achieving navigation accuracy within a range of 100 meters [17], [18], [21], [27].

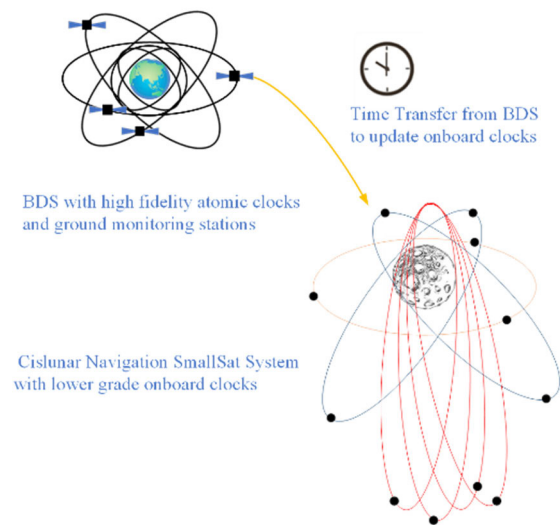


FIGURE 2. Time transfer from BDS to LNSS (not to scale) [19].

The format navigation message of the BDS B3I signal [28] contains essential navigation information parameters related to timing, including fundamental navigation information of broadcasting satellites (satellite ephemeris parameters, satellite autonomous satellite health flag (SatH1) & satellite health information (Heai), Age of Data Clock (AODC), Clock Correction Parameters (toc, a0, a1, a2) and their age and equipment group delay differential), almanac and BDT offsets from alternative systems, including UTC and other navigation satellite systems.

- **SatH1 & Heai.** The availability of the satellite is judged by extracting the SatH1 and Heai in the ephemeris. If not available, the time information of the satellite is removed. SatH1 (the autonomous satellite health flag) occupies 1 bit. “0” indicates that the broadcasting satellite is healthy and “1” indicates it is not. Heai (the satellite health information) requires 9 bits. The 9th bit indicates the health status of the satellite clock, while the 6th bit indicates the status of the B3I signal. Heai ($i = 1 \sim 30$) corresponds to the health information of satellites with IDs ranging from 1 to 30.

- AODC. Using the clock data age, the satellites whose clock difference data age is too long are eliminated. AODC is the extrapolation time interval of the clock error parameter.

It represents the difference between the reference time of the clock error parameter and the time of the last observation when the clock error parameter was calculated. This parameter is updated at the start of each hour in BDT. If $AODC < 25$, it indicates the age of the satellite clock correction parameters in hours. Considering the accuracy, we choose BDS satellites with $AODC < 25$ for timing.

- Clock Correction Parameters (t_{oc} , a_0 , a_1 , a_2). Updates are typically made hourly and at the commencement of BDT hours. t_{oc} , defined as integral points, represents the benchmark time for clock parameters in seconds.

- The equipment group delay differential. The inclusion of the B3I equipment group delay in the a_0 clock correction parameter eliminates the necessity for additional adjustments for users of the single-frequency B3I.

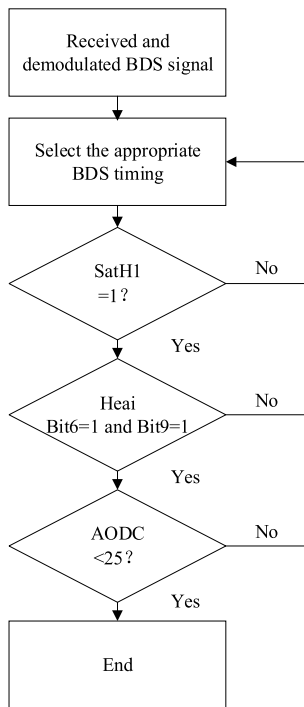


FIGURE 3. The appropriate processing flow of BDS timing signal.

Through the method in Fig.2, we can obtain BDS time signal that meets the timing requirements. Through calculation, the time information in the BDS signal can be obtained, and the time correction of the small satellite navigation constellation on the earth-moon orbit can be performed to improve the limited accuracy of the star clock. The BDS time computation is as follows [28]:

The user is able to compute BDT at time of signal transmission as:

$$t = t_{sv} - \Delta t_{sv} \quad (1)$$

In (1), t is BDT in seconds during signal transmission; t_{sv} is the actual phase time of the satellite’s ranging code in seconds

at the moment of signal transmission; Δt_{sv} is the deviation of the satellite’s ranging code phase time in seconds, as defined by the equation:

$$\Delta t_{sv} = a_0 + a_1(t - t_{oc}) + a_2(t - t_{oc})^2 + \Delta t_r \quad (2)$$

In (2), regardless of its sensitivity, t can be substituted with t_{sv} . Δt_r serves as the adjustment factor for the BDS satellite’s relativistic impact, characterized by

$$\Delta t_r = F \cdot e \cdot \sqrt{A} \cdot \sin E_k \quad (3)$$

In (3), e is the eccentricity of the BDS satellite’s orbit, as indicated by the broadcasting satellite’s ephemeris; A is the square root of the BDS satellite’s semi-major axis, also shown in the satellite’s ephemeris; E_k is eccentric anomaly in the BDS satellite’s orbit, also shown in the satellite’s ephemeris; $F = -2\mu^{1/2}/C^2$; $\mu = 3.986004418 \times 10^{14} \text{ m}^3/\text{s}^2$, is the geocentric gravitational constant values; $C = 2.99792458 \times 10^8 \text{ m/s}$, is the speed of light.

B. LNSS

Given that the initiatives for the lunar PNT constellation are in their initial design stage, the design of a LNSS necessitates finalizing numerous crucial design considerations, encompassing earth-moon navigation orbits and onboard clock.

1) EARTH-MOON NAVIGATION ORBITS

A variety of lunar trajectories have been explored before, such as the NRHO, DRO, and ELFO. NRHOs, characterized by their pronounced elliptical orbits, maintain almost steady visibility of the Earth and the moon’s poles. The DRO orbit is relatively stable and can provide continuous coverage of the moon, making it well-suited for navigation satellites. Specifically, ELFOs are a unique type of frozen orbits known for their superior lunar pole coverage. Orbits in a frozen state preserve stable orbital characteristics over prolonged durations, eliminating the need for station maintenance.

2) CRTBP AND LIBRATION POINTS ORBITS

The restricted three-body problem is the fundamental aerospace dynamics problem for investigating libration points in celestial mechanics. Within the Earth-Moon system, the spacecraft’s behavior is largely shaped by the gravitational pull from both the Earth and Moon, leading to the Three-Body Problem (TBP). Due to its inherent complexity, accurate solution of the three-body problem is challenging and often simplified as a Circular Restricted Three-Body Problem (CRTBP). A libration point refers to a location where a small celestial body experiences gravitational equilibrium between two larger celestial bodies. At this point, the small object remains nearly still in relation to the two main objects. Within the Earth-Moon system, investigating the restricted three-body problem in celestial mechanics yields five distinct solutions. In 1767, Swiss mathematician Euler calculated the first three collinear libration points L1, L2, and L3 lying along an axis connecting both main bodies.

In 1772, French mathematician Lagrange proved that there are two additional triangular points L4 and L5 located within an equilateral triangle formed by both main bodies.

In CRTBP, the equation of motion of the satellite in the syzygy frame is

$$\ddot{x} - 2\dot{y} = \frac{\partial U}{\partial x}, \quad \ddot{y} - 2\dot{x} = \frac{\partial U}{\partial y}, \quad \ddot{z} = \frac{\partial U}{\partial z} \quad (4)$$

In (4), (x, y, z) is the position of the satellite, $(\dot{x}, \dot{y}, \dot{z})$ is the velocity, $(\ddot{x}, \ddot{y}, \ddot{z})$ is the acceleration, U is the equivalent potential energy with value of

$$U = \frac{1}{2}(x^2 + y^2) + \frac{1 - \mu}{d_1} + \frac{\mu}{d_2} + \frac{1}{2}\mu(1 - \mu) \quad (5)$$

In (5), $d_1 = [(x + \mu)^2 + y^2 + z^2]^{1/2}$ and $d_2 = [(1 - x - \mu)^2 + y^2 + z^2]^{1/2}$ are the distances between the spacecraft and the two major celestial bodies, respectively.

$$\mu = \frac{M_2}{M_1 + M_2}, \quad 1 - \mu = \frac{M_1}{M_1 + M_2} \quad (6)$$

In (6), M_1 and M_2 are the masses of the Earth and the Moon, respectively. The distances of the principal objects M_1 and M_2 to the origin of the syzygy frame are μ and $1 - \mu$, respectively.

$$JC = 2U - \dot{x}^2 - \dot{y}^2 - \dot{z}^2 \quad (7)$$

In (7), JC is the Jacobi integration constant that characterizes the energy of the spacecraft, with a larger JC indicating less energy.

The process of differential correction is employed to adjust a set of initial conditions in order to meet specific criteria. For instance, in targeting problems, differential correction is utilized when a desired final position is specified or when modifying the initial conditions to accommodate variations in system attributes. The effectiveness of differential correction relies on the utilization of the state transition matrix (STM), which facilitates mapping from the initial condition to the final state at a given time. To commence describing the STM (State Transfer Matrix), it is necessary to define a state vector in (8).

$$\mathbf{X} = [x \quad y \quad z \quad \dot{x} \quad \dot{y} \quad \dot{z}] \quad (8)$$

The STM is in (9) then,

$$\Phi(t, t_0) = \frac{\partial \mathbf{X}(t)}{\partial \mathbf{X}(t_0)} = \begin{bmatrix} \Phi_{rr} & \Phi_{rv} \\ \Phi_{vr} & \Phi_{vv} \end{bmatrix} \quad (9)$$

- NRHO. NRHO is a recurring trajectory within the halo orbit family, centered around the L1/L2 point in a tripartite system. Typically, this orbit is markedly elliptical within the circle-constrained three-body problem (CR3BP) at the Earth-Moon L2 point, representing a unique instance of the halo orbit around L1/L2 in the Earth-Moon system. NRHOs exhibit advantageous dynamic and geometric characteristics, ensuring near-steady visibility from Earth and uninterrupted surveillance of the Moon's Antarctic area. This feature simplifies the management of the orbit from Earth and allows for surveillance of the Moon's south pole. As a result, it is

presently considered a viable orbital choice for upcoming crewed deep space stations. Consequently, it is currently regarded as a potential orbital option for future manned deep space stations. Various aspects related to NRHO orbits have been investigated, including Earth-NRHO transfers, station keeping techniques, and ground station visibility conditions. Reference [17] explored different sizes of NRHOs to avoid eclipses and verified their feasibility for Earth-Moon round-trip activities. Reference [27] designed an NRHO trajectory for lunar soft landing purposes while reference [29] analyzed its feasibility for orbital transfer to reach lunar surfaces. Furthermore, reference [30] analyzed the moon's visible states and its surroundings, including rough assessments of user receivers' performance while using NRHO orbits as navigational groups.

- DRO. Within the CRTBP model, the Distant Retrograde Orbit (DRO) group is part of a unique symmetric planar family. With rising amplitudes, Earth's impact intensifies, leading to a greater divergence of the DRO's shape from a circular trajectory. If DROs are near the Moon, the Earth's impact diminishes, leading them to move in retrograde circular trajectories around the Moon within a dual-body framework. Consequently, fewer orbit control maneuvers are required due to this behavior. The planar DROs lie within the Moon's orbital plane and provide extensive coverage of its surface except for polar regions. The citation [31] indicates that DRO orbits provide more stability than Collinear Libration Point (CLP) orbits, making them better suited for navigational use. For encompassing lunar polar areas, Reference [32] implemented a minor adjustment in out-of-plane amplitude for planar DROs. Additionally, Reference [33] proposed a high-precision dynamic model with a simple structure specifically designed for deep space navigation and communication applications.

3) ELFO

Frozen orbits, marked by steady average eccentricity, mean inclination, and mean argument of perigee, are widely utilized in various space applications [34]. The gravitational field's north-south imbalance results in satellites circling the Earth and Moon moving in motion. A frozen orbit is a stable orbit that maintains constant eccentricity and perigee amplitude. When fixing the semi-major axis and inclination of an orbit, there exist infinitely many orbits with only one frozen orbit. The complex gravitational field of the Moon results in distinct characteristics for lunar satellite orbits compared to those around Earth [35]. Lunar satellites do not experience atmospheric drag or decay in their orbits due to the absence of atmosphere on the Moon; hence, there is no decrease in semi-major axis or concern about orbital lifetime as observed with Earth satellites. Generally speaking, for probes circling the Moon, primary disturbances arise from both its gravitational field (the main body) and third bodies (such as Earth). For lower altitude orbiter missions, moon-induced gravity field disturbances significantly impact eccentricity

and perigee amplitude. Lunar satellites operating at lower altitudes may eventually descend onto the lunar surface after a certain period of time. Given its importance in navigation applications, numerous studies have designed lunar navigation constellations based on frozen orbits. In particular, Elliptical Lunar Frozen Orbit (ELFO) refers to a specific type of frozen orbit that offers broader coverage over lunar poles [36]. The frozen orbit refers to a long-term stable orbit with minimal orbital maintenance, maintaining almost constant orbital parameters. According to Reference [37], the moderate altitude frozen orbit exhibits slight oscillation in eccentricity near its initial value, while the inclination remains nearly constant, making it stable and suitable for navigation purposes. Reference [38] suggests that freezing orbits can enable 20 satellites to form highly efficient lunar GNSS constellations; however, this approach is not ideal for high latitudes. Optimal navigation performance is achieved when the inclination is approximately 40 degrees. In consideration of two different configurations of the ELFO constellation discussed in Reference [26], both configurations have an inclination of 63°, with one focusing on the Antarctic region and the other on the Moon's Arctic region.

As the Earth-Moon navigation system's reference satellite, LNSS maintains the accuracy of its onboard clock by synchronizing with the visible arc of BDS and provides navigation services for lunar surface and near-lunar space. To investigate LNSS's navigation performance, it is essential to establish an effective simulation framework. In this study, we assume an omnidirectional antenna for transmitting navigation signals from LNSS. Subsequently, factors such as half-cone size, transmission power, and signal propagation attenuation are taken into account. The LNSS constellation comprises various satellite orbit types introduced in Section II-A (including DRO, NRHO, and ELFO). For our simulation case, we set up an Earth-Moon rotating frame, where the barycenter between Earth and Moon served as the coordinate starting point. The X-axis coincides with the instantaneous Earth-Moon position vector, whereas the Z-axis is in sync with the instantaneous angular momentum vector of the Moon's orbit around Earth; completing this orthogonal system is the Y-axis. We employed a high-precision orbit propagator (HPOP) to numerically calculate these satellites' orbits within the Earth-Moon orbit considering precise force models for Earth, Sun, and Moon; thereby generating and propagating accurate position and velocity solutions for satellites in the Earth-Moon orbit.

After initial attempts, constellations with configurations such as D2N3, D2N4, D3N2, D3N3, and D4N2 exhibit inadequate satellite coverage in the southern hemisphere of the Moon and fail to meet navigation performance requirements. The region covered by the D3N4 configuration only satisfies conditions within the range of the Moon South Pole region but exhibits weaker coverage in the mid-latitude area of the Southern Hemisphere. By minimizing additional ELFO satellites while ensuring sufficient coverage, it is possible to achieve satisfactory navigation design requirements for

the southern hemisphere of the moon. To this end, we have selected 6 and 8 ELFO satellites with 2 symmetrical orbital planes to form constellations of D3N4E6 and D3N4E8 for comparative analysis.

The established configurations of LNSS constellations are presented in Table 2, while their navigation performance is compared and analyzed in the experimental results discussed in Section III.

TABLE 2. Satellite orbit selection of LNSS constellation.

LNSS	DRO	NRHO	ELFO
D3N4	DRO_0	NRHO_0	—
	DRO_33	NRHO_25	
	DRO_66	NRHO_50	
		NRHO_75	
D3N4E6	DRO_0	NRHO_0	ELFO_0(3) ELFO_180(3)
	DRO_33	NRHO_25	
	DRO_66	NRHO_50	
		NRHO_75	
D3N4E8	DRO_0	NRHO_0	ELFO_0(4) ELFO_180(4)
	DRO_33	NRHO_25	
	DRO_66	NRHO_50	
		NRHO_75	

4) SATELLITE CLOCK IN SMALLSAT PLATFORM

For future lunar-orbiting satellites, the payload capacity of the small satellite platform imposes limitations on the performance of the onboard clock. Our study focuses on simulating a star clock for small satellite platforms using a compact and low-power Microchip Atomic Clock (MAC). The detailed parameters of this clock are presented in Table 3. To accurately model clock errors in short-term data fitting, we employ a widely-used quadratic polynomial model.

$$\sigma_{clk} = b_0 + b_1(t - t_0) + b_2(t - t_0)^2 + \Delta t_\delta \quad (10)$$

TABLE 3. The onboard clock characteristics and parameters.

Size (cm ³)	Weight (kg)	Power (W)	Onboard clock parameters			
			b_0	b_1	b_2	Δt_δ
30	1	0.5	2.82 ×10 ⁻⁵	3.56×10 ⁻¹²	2.76×10 ⁻¹⁹	rand×1 0 ⁻¹¹

In (10): σ_{clk} is the clock difference at time t . At the reference time of the atomic clock t_0 , b_0 is the clock error, b_1 is the clock speed, b_2 is the clock drift, and Δt_δ is the random error.

The update of the LNSS onboard clock relies on the communication between the LNSS satellite and BDS satellite. When there is intervisibility between the LNSS and BDS satellites, it is deemed feasible to utilize BDS time transfer for updating the low-precision satellite clock of LNSS.

However, continuous updates are not necessary in all cases when visibility exists.

C. LNSS LUNAR SURFACE AND LLO

We investigate the navigation performance of LNSS by considering lunar surface and LLO satellites as illustrative examples. For the lunar surface, we partition it into grids based on 1° × 1° latitude and longitude intervals, focusing on analyzing the coverage of each grid point in terms of the number of LNSS satellites, as well as evaluating the DOP and navigation accuracy at each grid point. Furthermore, a LLO satellite is chosen to represent user satellite within the LNSS constellation for assessing its navigation performance. The orbital parameters for this LLO satellite are presented in table 4. By examining various LLO orbits, we determine that receiving LNSS navigation signals is feasible whenever a visible connection with a LNSS satellite exists. In our subsequent research endeavors, we will consider factors such as antenna direction and signal half cone angle.

TABLE 4. Orbital parameters of LLO.

satellite	Epoch (UTC)	<i>a</i> (km)	<i>e</i>	<i>i</i>	ω	Ω	λ
LLO	1Jan 2026 00: 00: 00.000	2500	0.2	90	85	128	0

III. EXPERIMENTAL RESULTS AND ANALYSIS

A. VALIDATION METRICS

To fulfill the accuracy requirements for Earth-Moon space navigation, it is essential to update the LNSS onboard clock with BDS time within a reasonable timeframe in order to enhance its clock accuracy. The optimal solution should strike a balance between maximizing satellite visibility, minimizing maximum continuous invisibility, and maintaining UERE (User Equivalent Ranging Error) and DOP accuracy requirements reasonably. To facilitate comparative studies in this research, we established these four criteria for validation:

- **Satellite visibility.** Satellite visibility is the percentage of time in which the number of BDS satellites visible exceeds the predetermined threshold throughout the experiment. Satellite visibility satisfies two conditions: a) the minimum requirement for estimating clock bias and drift is met by ensuring that at least one BDS satellite is visible for a certain percentage of time; b) to include satellite position and velocity, satellite clock deviation and drift, it is necessary to ensure that at least four BDS satellites are visible for a certain percentage of time.

- **Maximum Continuous Invisible (MCI).** MCI is the maximum continuous duration for which LNSS satellites and BDS satellites lose visibility. During MCI, the satellites of LNSS and BDS are not visible and cannot transfer timing. The satellite clock of LNSS will have a cumulative error that affects navigation accuracy.

- **Multiple coverage.** Multiple coverage represents the number of LNSS navigation satellite signals available at any given point on the lunar surface and LLO orbit. A higher value of Multiple coverage indicates a greater availability of navigation satellites at that time. The indicators of GDOP are not well-suited for measuring the navigation performance in specific orbits within the unique dynamic environment of the Lunar Navigation System. Therefore, we utilize multiple coverage and UERE as two metrics to analyze the performance of navigation constellations. GDOP is highly suitable for characterizing geometric positioning accuracy in traditional surround orbit type constellations. However, when using fewer satellites to achieve an equivalent function compared to traditional surround orbit constellations, the calculated value of GDOP metric becomes excessively large; nevertheless, this does not imply suboptimal navigation accuracy.

- **UERE.** the UERE metric is used to assess the accuracy of LNSS satellite’s navigational signals for users on the lunar surface and near-lunar space. As mentioned earlier in Section III-C, the lunar UERE depends on the RMS error in clock bias. In this study, we propose a lunar UERE metric specifically tailored to characterize the ranging accuracy of LNSS signals in these unique environments. Unlike Earth’s atmosphere, both atmospheric delay and ionospheric delay can be disregarded on the moon’s surface and near-moon space. Furthermore, due to the absence of tall buildings and relatively flat water bodies, multipath effects can also be neglected. Therefore, we calculate LNSS’s UERE using four key error components as follows:

$$\sigma_{UERE, CLNSS} = \sqrt{\sigma_{clk}^2 + \sigma_{gd}^2 + \sigma_{eph}^2 + \sigma_{rec}^2} \quad (11)$$

In (11), σ_{clk} is the LNSS clock error, σ_{gd} is the differential group delay caused by the LNSS signal structure, σ_{eph} is the broadcast ephemeris, and σ_{rec} is the receiver noise caused by the lunar user receiver.

B. SATELLITE VISIBILITY AND MCI ANALYSIS

1. The number of visible BDS satellites on the three types of orbits considered in our case study during the simulation experiment time is illustrated in Figs. 3a-3d.

2. Based on Tab.5, it can be observed that the satellites in NRHO and DRO orbits are visible to the BDS constellation throughout the entire duration of the experiment, satisfying both experimental conditions of at least one and at least four satellite visibility without any MCI time interval.

TABLE 5. Comparison analysis across different orbit types.

Orbit Type	Max MCI (s)		Satellite Visibility (%)	
	≥1	≥4	≥1	≥4
NRHO	0.000	0.000	100%	100%
DRO	0.000	0.000	100%	100%
EFLO	3043.7	3402.2	99.50%	99.39%

3. The conclusion regarding NRHO is reasonable as these satellites operate at a high altitude between 4500 km and 700,000 km from the Moon's surface, resulting in less occultation from both Earth and Moon.

4. Similarly, DRO orbit exhibits similar orbital characteristics away from the moon. Therefore, NRHO and DRO orbits are highly suitable for constructing LNSS navigation systems utilizing BDS for time transfer.

5. However, EFLO orbit shows that with at least one satellite visibility with BDS satellites, there exists a Max MCI of 3043.7s which accounts for 99.50% of total visibility duration; when communicating with at least four BDS satellites, there exists a Max MCI of 3402.2s which represents 99.39% of total visibility duration.

6. Although ELFO orbit has relatively high altitude position, it still experiences block-age by the moon hindering reception of BDS signals required to maintain LNSS's satellite clock synchronization.

7. According to analysis results obtained from satellite visibility and MCI evaluation outcomes, it can be concluded that LNSS and BDS remain almost continuously visible. Therefore, it is feasible to utilize high precision satellite clocks provided by BDS for time synchronization services within LNSS.

C. IMPROVEMENT OF THE ACCURACY OF STAR CLOCK AFTER TIMING

Using the satellite clock in Section III-C as an example, we validate the efficacy of BDS timing by comparing the navigation accuracy of LNSS before and after implementing BDS timing. Our focus is on an LNSS satellite fitted with a BDS receiver and an integrated clock, ensuring stable timing over a short period. The intermittent availability of BDS signals is utilized to update the LNSS satellite clock, while the lunar UERE metric in Section 4.1 is developed to define the accuracy of transmitted navigational signals. To maintain accurate LNSS star clocks, our clock propagation model performs time updates every T_{pred} second. The transmit power and antenna gain model for L1 C/A signal from earth-GPS satellites can be found in Reference [39]. Additionally, Reference [40] proposes a transmitting antenna model for BDS signals in earth-moon space which we adopt to establish the LNSS receiver antenna model. In order to maximize visibility of BDS signals on the LNSS satellite, we simulate a space-borne Earth-BDS receiver with an antenna pointing towards Earth based on research findings [41] that demonstrate receiving and usability conditions for BDS in earth-moon space. For simulation simplicity, it is assumed that the BDS satellite is visible from the perspective of LNSS. Finally, we introduce simulated clock bias and drift into real distance and distance rate between BDS and LNSS satellites to simulate received measurements on the LNSS satellite.

In our current study, we investigated the impact of the onboard clock's LNSS clock error component σ_{clk} on various Earth-Moon orbits and analyzed how different satellite

clock orbits affect the overall moon UERE before and after BDS timing. Additionally, we examined the influence of observation update rate on lunar UERE when BDS signal is available, with a sampling period denoted as T_{pred} seconds. Notably, larger values of T_{pred} result in less frequent BDS measurement updates, enabling longer standby periods for energy conservation purposes.

In order to characterize the UERE on the lunar surface and near-moon space, the group delay and receiver noise error magnitudes we utilize are identical to those employed in the BDS, namely $\sigma_{gd} = 0.20$ m and $\sigma_{rec} = 0.15$ m. Considering that China Lunar Navigation Support System (LNSS) imposes stricter requirements on ground monitoring infrastructure compared to BDS in future scenarios, we conduct a case study by scaling up the error component of broadcast ephemeris for lunar UERE to $\sigma_{eph} = 3$ m. The value of σ_{clk} is calculated according to Formula (10). This value is one order of magnitude higher than that of BDS. To meet the accuracy requirements for LNSS satellite clocks, we design a timing filter with T_{pred} parameter representing the update time interval set at $T_{pred} = 60$ s. Fig.4 shows a simulation experiment lasting for 600 seconds, where BDS timing with an interval of 60 seconds can essentially satisfy the error accuracy demands.

D. CASE ANALYSIS FOR MOON

In order to assess the navigation performance of LNSS on the lunar surface, an analysis was conducted on the satellite navigation signal multi-coverage range across the entire moon, and the navigation accuracy of LNSS for the entire moon was evaluated. For simulation purposes, considering computational constraints, a grid size of $1^\circ \times 1^\circ$ based on latitude and longitude steps was employed to represent the entire lunar region, with a simulation time step set at 300 seconds. The experimental duration was set at 30 days.

TABLE 6. Simulation settings of case analysis for moon.

Parameter	values
step in latitude and longitude for lunar	1°
time step in the simulation	3600s
multiple coverage	0~15
uncertainty in the range of the LNSS sensor	5m
uncertainty in the range of the moon's surface receiver	5m
time transfer	BDS
ephemeris	JPL-DE430
earth rotation parameters	IERS04

- Multiple coverage analysis. As depicted in Figure 5, during the 30-day simulation experiment, LNSS effectively covered the southern hemisphere of the moon. However, in certain areas north of 15°S , the multiple coverage achieved by D3N4 is limited to only 3.98, whereas both D3N4E6 and D3N4E8 can achieve a coverage of 5 or more. In regions south of 30°S , their coverage extends to 8 and 10 respectively. This discrepancy arises due to longer stay times at the South Pole for satellites in southbound NRHO and ELFO orbits, resulting in increased navigation service time.

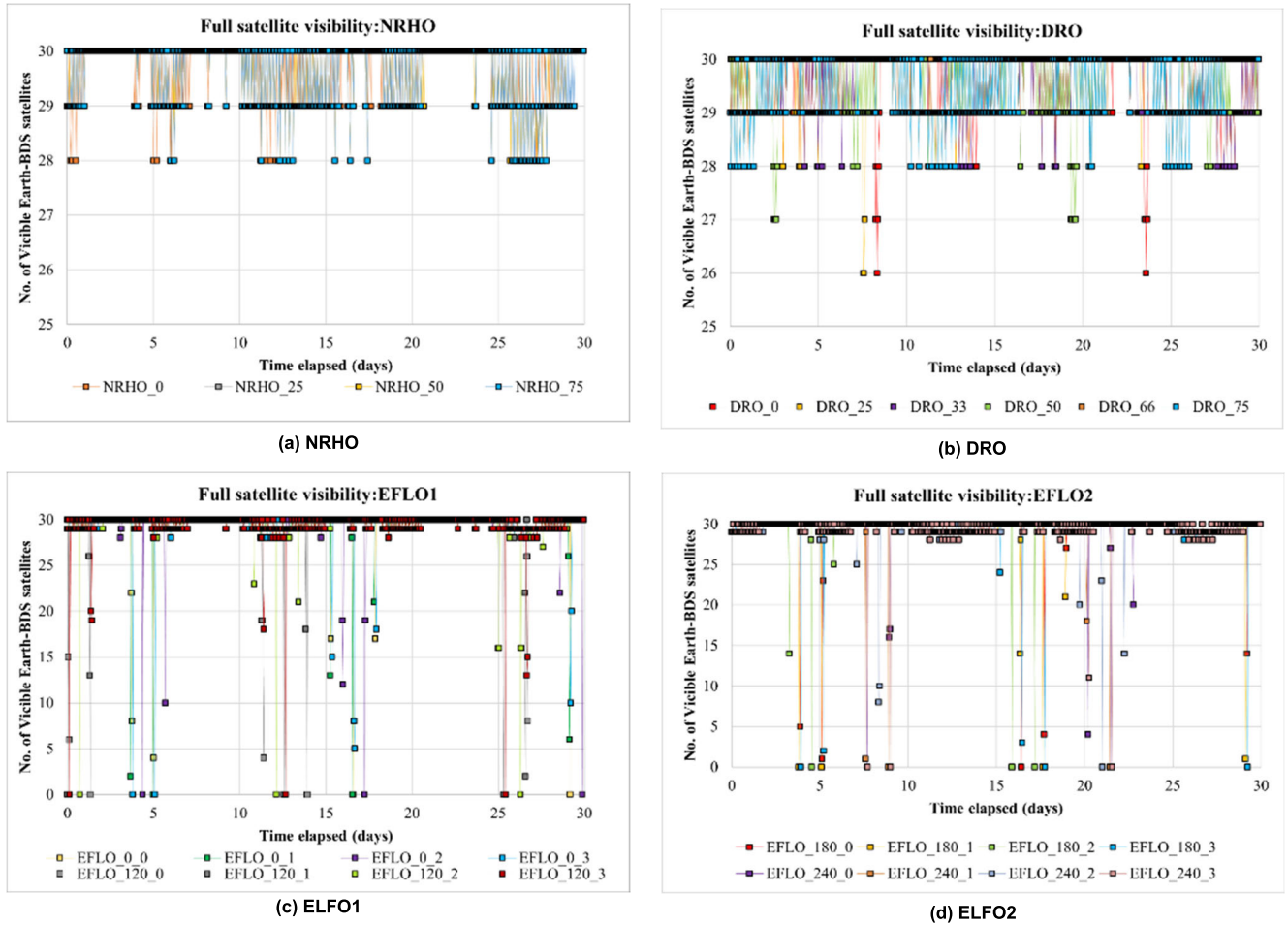


FIGURE 4. BDS satellite visibility across different orbit types.

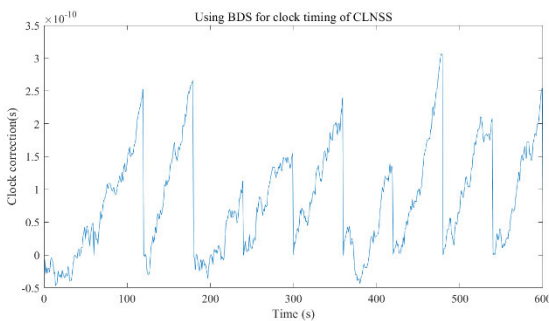


FIGURE 5. Using BDS for clock timing of LNSS.

The performance of LNSS in providing coverage within the lunar Arctic region is suboptimal. To establish a navigation constellation with complete lunar coverage, it may be necessary to consider incorporating satellites in north-bound NRHO orbits to enhance multiple coverage within this Arctic region.

- **Navigation Accuracy.** In the simulation, the range uncertainty of the satellite sensor of the LNSS is set to 5m, and the range uncertainty of the lunar surface receiver is also

set to 5m. The navigation accuracy of the LNSS for lunar missions is illustrated in Figure 6. Specifically, in areas south of 30°S on the Moon, the navigation accuracy reaches below 40 meters. While D3N4 alone can meet these requirements within this specific area, considering future exploration missions expanding across the southern hemisphere of the Moon necessitates extending activity coverage to encompass its entirety and incorporating ELFO orbiting satellites into the constellation. Notably, there is no significant difference in navigation accuracy between D3N4E6 and D3N4E8 constellations; however, adhering to a principle that minimizes satellite numbers makes using D3N4E6 more advantageous.

According to the aforementioned analysis, during a 30-day simulation experiment, D3N4 achieved a minimum of four-time coverage and complete navigation signal coverage (100%) in the lunar region located south of 30°S. Both D3N4E6 and D3N4E8 of LNSS also attained at least four-time coverage, with respective capabilities reaching eight and ten in areas south of 30°S. The navigation accuracy of D3N4 generally satisfies the requirements for lunar surface navigation south of 30°S, while there is no significant difference in navigation accuracy between D3N4E6 and D3N4E8;

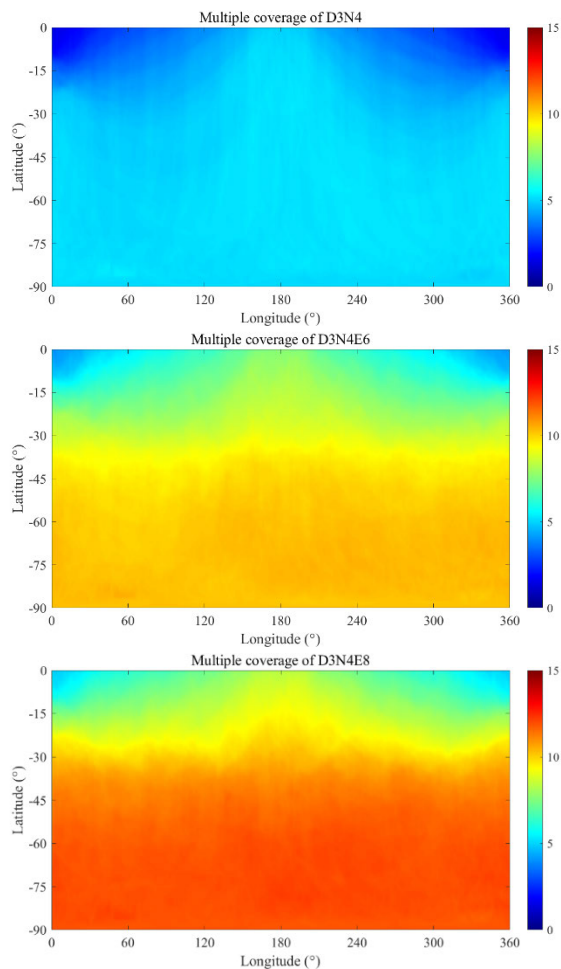


FIGURE 6. Multiple coverage of LNSS to moon.

both can essentially meet the demands for southern hemisphere lunar surface navigation. However, certain regions on the lunar surface still exhibit relatively low navigation accuracy due to limited satellite availability from LNSS during specific periods. This situation can be improved by increasing the number of northbound NRHO satellites.

E. CASE ANALYSIS FOR LLO

In this study, we employ a Low Lunar Orbit (LLO) satellite as the user to evaluate the navigation performance of Cooperative Lunar Navigation Satellite System (LNSS) in proximity to lunar space range. Through simulation experiments, which are detailed in Table 7, we comprehensively analyze the navigation capabilities of LLO utilizing LNSS for both coverage and accuracy.

- **Multiple coverage analysis.** The real-time coverage effect of three configurations of the LNSS navigation signal on the LLO orbit is depicted in Figure 7 within a span of 30 days. While D3N4 demonstrates satisfactory performance south of 30°S, it falls short in achieving quadruple coverage across numerous orbital segments north of this latitude. By incorporating ELFO orbit satellites into the constellation,

TABLE 7. Simulation settings of case analysis for LLO.

Parameter	values
satellite	LLO
integration step	3600s
uncertainty in the range of the LNSS sensor	5m
uncertainty in the range of the LLO receiver	5m
time transfer	BDS
ephemeris	JPL-DE430
earth rotation parameters	IERSC04

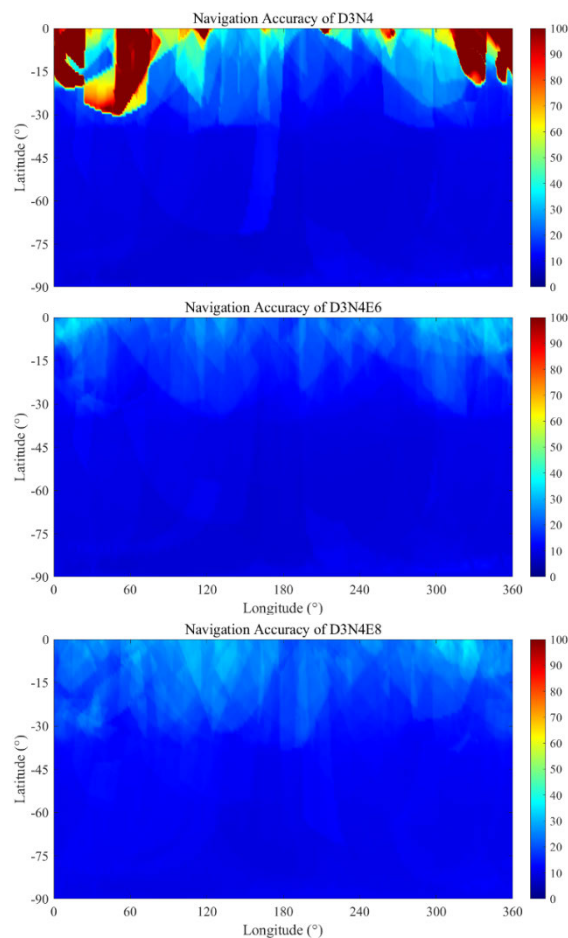


FIGURE 7. Analysis of navigation accuracy for moon.

multiple coverage capabilities can be enhanced for navigation satellites operating in middle and low latitudes on the Moon. Both D3N4E6 and D3N4E8 fulfill the requirement for multiple coverage; however, D3N4E6 offers economic advantages with fewer satellites. In regions south of 60°S on the lunar surface as well as in low orbit spaces within the southern hemisphere involved in lunar exploration expansion missions, activation of LLO satellite payload plays a crucial role in observing these areas. The navigation signal coverage range provided by the D3N4E6 configuration LNSS exceeds ten, thereby meeting all requirements.

- **Navigation Accuracy.** In this test, both the range uncertainty of LNSS satellite transmitter and LLO satellite receiver are set to 5m. The measurable flight segments of LLO with

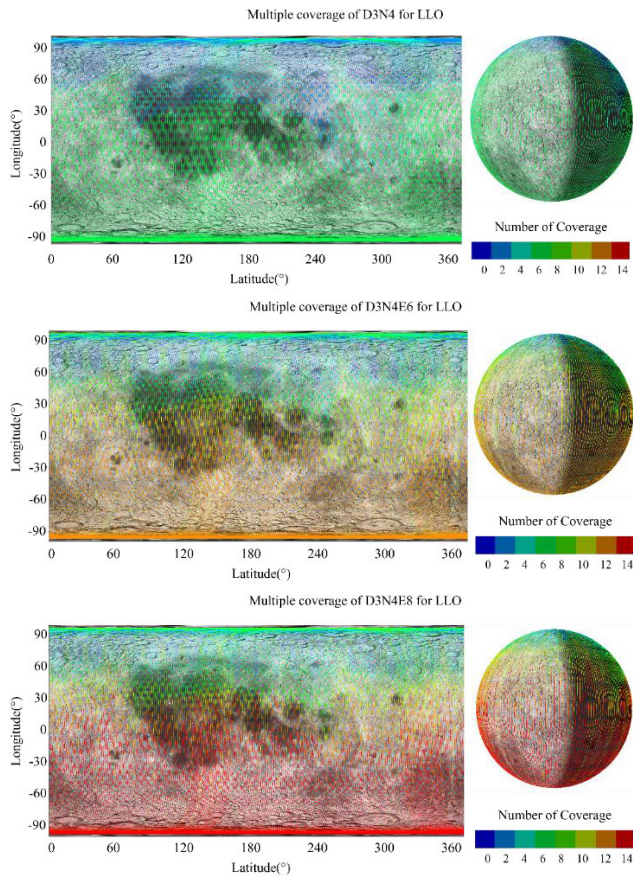


FIGURE 8. Multiple coverage of LNSS for LLO.

navigation accuracy above 100 meters account for 98.9%. Fig.8 shows the navigation accuracy of three constellations of LNSS for LLO orbit satellites. For D3N4, the navigation accuracy in south of 30°S meets the requirements, but due to limited number of LNSS satellites, some orbital segments in areas north cannot be navigated. However, after adding ELFO satellites, this situation has improved significantly. The navigation accuracy performance of D3N4E6 and D3N4E8 is similar with most LLO orbit segments having a navigation accuracy exceeding 100 meters in some orbital segments north of 60°N and within 100 meters for most other orbital segments including those that account for over 98% measurable flight segment meeting design requirements.

According to the aforementioned analysis, the LNSS employing the D3N4 configuration can offer satellite navigation support for the orbital segment located south of 30°S of the LLO satellite. Furthermore, by utilizing the LNSS with a D3N4E6 configuration, navigation accuracy support up to 100 meters can be achieved for the orbital segment situated south of 60°N of the LLO satellite.

IV. DISCUSSION

The current study demonstrates that the utilization of LNSS with Time-Transfer from BDS could serve as a viable and

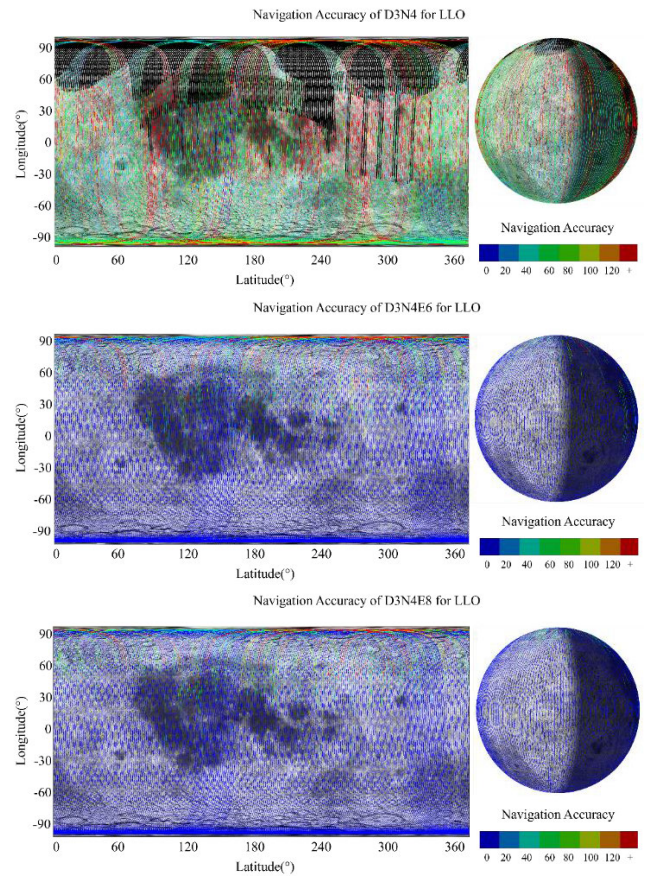


FIGURE 9. Analysis of navigation accuracy for LLO.

cost-effective approach for Moon Navigation in the Southern Hemisphere. This method has successfully achieved navigation near the Moon South Pole with a reduced number of satellites. LNSS fulfills the design requirements for providing multiple coverage and ensuring Navigation Accuracy in the southern hemisphere of the moon, thereby effectively supporting future lunar exploration missions.

The experiments conducted in our study have specifically chosen DRO, NRHO, and ELFO satellite orbits for LNSS. Within the LNSS framework, satellites positioned in DRO and NRHO orbits ensure consistent visibility with BDS, thereby guaranteeing high-precision time transfer. Although satellites located in ELFO orbit may encounter occasional lunar obstructions, their overall visibility remains above 99%. The integration of the D3N4 configuration with DRO and NRHO effectively fulfills the requirements for lunar regions below 15°S. For surface operations on the Moon, a minimum of four overlapping coverage areas are achieved with navigation accuracy within 100 meters. Similarly, for LLO orbit segments situated above the lunar south of 15°S, multiple coverage and navigation accuracy align with design specifications. However, it should be noted that the D3N4 configuration does not adequately cater to lunar regions north of 15°S. In anticipation of potential future exploration

missions extending beyond the South Pole region of the Moon, we have introduced ELFOs into our constellation to enhance satellite coverage across the southern hemisphere northward from 15°S. As a result, our newly proposed D3N4E6 configuration successfully meets all design requirements.

In our experimental simulation, we assume that the LNSS satellite can effectively receive BDS satellite signals for precise timing transfer. Additionally, the LNSS satellite is capable of transmitting navigation signals to facilitate reception by lunar surface users and LLO satellite users. To ensure higher accuracy in near real effect results, an accurate spatial transmission attenuation model for signal propagation will be employed. Currently, only omnidirectional antennas are being considered; however, future work should focus on assessing how antenna directionality influences navigation signal reception by considering factors such as antenna direction and signal half cone angle.

In this paper, our focus lies in establishing a regional satellite navigation constellation design specifically tailored for the southern hemisphere of the Moon, with the primary objective being to prioritize exploration of the South Pole region. However, it should be noted that this particular constellation design may not be optimal for ensuring efficient navigation performance in the northern hemisphere of the Moon. The coverage provided by LNSS within the lunar Arctic region is currently suboptimal; therefore, to achieve complete lunar coverage and enhance multiple coverage within this Arctic region, it may be necessary to consider incorporating satellites in north-bound NRHO orbits. Additionally, further research is required to optimize the phase between various orbital planes and satellites within the constellation configuration, thereby making it more reasonable.

V. CONCLUSION

This paper designs and examines the LNSS architecture that utilizes BDS time transfer. It conducts a comprehensive analysis of the diverse orbit traits and navigational attributes. An analysis is conducted on the visibility of various satellite orbit types and their maximum continuous invisibility to BDS. Furthermore, a detailed examination is carried out on the design of LNSS using BDS time transfer to utilize BDS time transfer to enhance navigation precision in the lunar surface and low lunar space. This paper confirms the practicality and initial efficacy of LNSS employing BDS as time transfer, providing valuable insights for BDS and GNSS in delivering navigational services in lunar space. The D3N4 configuration effectively meets the requirements of lunar areas below 15°S. At least four-time coverage can be achieved on the lunar surface and in the LLO orbital segment above the southern moon, with a navigation accuracy of within 100 meters. Considering that future exploration missions may extend beyond the lunar south pole. The D3N4 does not fully meet the needs of lunar areas north of 15°S, with a multiple coverage range limited to 3.98. We have introduced ELFO into

the constellation to enhance satellite coverage from north areas of 15°S in the southern hemisphere. Both D3N4E6 and D3N4E8 can achieve a coverage range of 5 or greater. Notably, there is no significant difference in navigation accuracy between D3N4E6 and D3N4E8 constellations; however, adhering to the principle of minimizing the number of satellites makes using D3N4E6 more advantageous. A novel idea and approach towards lunar space navigation are proposed. The subsequent steps involve simulating earth-moon communication for BDS signals with enhanced realism, refining the configuration of the LNSS constellation, as well as focusing on supporting navigation performance for specific areas during future lunar exploration missions.

REFERENCES

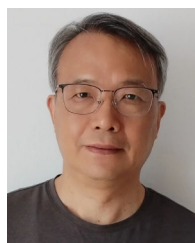
- [1] China Nat. Space Admin. (2021). *International Lunar Research Station (ILRS) Guide for Partnership*. [Online]. Available: <https://www.cnsa.gov.cn/english/n6465652/n6465653/c6812150/content.html>
- [2] C. Wang, Y. Lin, Z. Pei, Y. L. Zou, L. Xu, H. H. Cheng, J. Ren, and C. Yu, "Key scientific questions related to the lunar research station," *Bull. Nat. Natural Sci. Found. China*, vol. 36, no. 6, pp. 830–840, 2022.
- [3] T. Hu, Z. Yang, M. Li, C. H. van der Bogert, Z. Kang, X. Xu, and H. Hiesinger, "Possible sites for a Chinese international lunar research station in the lunar south polar region," *Planet. Space Sci.*, vol. 227, Mar. 2023, Art. no. 105623.
- [4] C. Li, C. Wang, Y. Wei, and Y. Lin, "China's present and future lunar exploration program," *Science*, vol. 365, no. 6450, pp. 238–239, Jul. 2019.
- [5] X. Zeng, D. Liu, Y. Chen, Q. Zhou, X. Ren, Z. Zhang, W. Yan, W. Chen, Q. Wang, X. Deng, H. Hu, J. Liu, W. Zuo, J. W. Head, and C. Li, "Landing site of the Chang'e-6 lunar farside sample return mission from the Apollo basin," *Nature Astron.*, vol. 7, no. 10, pp. 1188–1197, Jul. 2023.
- [6] X. Zeng and D. Liu, "Where should Chang'e-6 collect samples on the farside of the Moon?" *Nature Astron.*, vol. 7, pp. 1158–1159, Jul. 2023.
- [7] C. Wang, Y. Jia, C. Xue, Y. Lin, J. Liu, X. Fu, L. Xu, Y. Huang, Y. Zhao, Y. Xu, R. Gao, Y. Wei, Y. Tang, D. Yu, and Y. Zou, "Scientific objectives and payload configuration of the Chang'e-7 mission," *Nat. Sci. Rev.*, vol. 11, no. 2, Jan. 2024, Art. no. nwad329.
- [8] Y. He, H. He, Z. Liu, F. Su, J. Li, Y. Zhang, R. Li, X. Huang, X. Zhang, C. Lu, S. Jiang, J. Tang, and R. Liu, "Proof of principle of the lunar soil volatile measuring instrument on Chang'e-7: In situ N isotopic analysis of lunar soil," *Aerospace*, vol. 11, no. 2, p. 114, Jan. 2024.
- [9] N. Liu and Y.-Q. Jin, "Selection of a landing site in the permanently shadowed portion of lunar polar regions using DEM and mini-RF data," *IEEE Geosci. Remote Sens. Lett.*, vol. 19, pp. 1–5, 2022.
- [10] G. Wei, X. Li, W. Zhang, Y. Tian, S. Jiang, C. Wang, and J. Ma, "Illumination conditions near the Moon's south pole: Implication for a concept design of China's Chang'e-7 lunar polar exploration," *Acta Astronautica*, vol. 208, pp. 74–81, Jul. 2023.
- [11] Y. Yang, X. Ren, X. Jia, and B. Sun, "Development trends of the national secure PNT system based on BDS," *Sci. China Earth Sci.*, vol. 66, no. 5, pp. 929–938, May 2023.
- [12] X. Ren and Y. Yang, "Development of comprehensive PNT and resilient PNT," *J. Geodesy Geoinf. Sci.*, vol. 6, no. 3, pp. 1–8, Sep. 2023.
- [13] S. Song, Z. Zhang, and G. Wang, "Toward an optimal selection of constraints for terrestrial reference frame (TRF)," *Remote Sens.*, vol. 14, no. 5, p. 1173, Feb. 2022.
- [14] L. Ma, Z. You, B. Li, B. Zhou, and R. Han, "Deep coupled integration of CSAC and GNSS for robust PNT," *Sensors*, vol. 15, no. 9, pp. 23050–23070, Sep. 2015.
- [15] D. A. Grejner-Brzezinska, C. K. Toth, T. Moore, J. F. Raquet, M. M. Miller, and A. Kealy, "Multisensor navigation systems: A remedy for GNSS vulnerabilities?" *Proc. IEEE*, vol. 104, no. 6, pp. 1339–1353, Jun. 2016.
- [16] C. Rizos and L. Yang, "Background and recent advances in the locata terrestrial positioning and timing technology," *Sensors*, vol. 19, no. 8, p. 1821, Apr. 2019.
- [17] S. Bhamidipati, T. Mina, and G. Gao, "A case study analysis for designing a lunar navigation satellite system with time-transfer from Earth-GPS," *Comput. Sci. Robot.*, vol. 21, pp. 1–13, Jan. 2022.

- [18] J. J. R. Critchley-Marrows, X. Wu, Y. Kawabata, and S. Nakasuka, "Autonomous and Earth-independent orbit determination for a lunar navigation satellite system," *Aerospace*, vol. 11, no. 2, p. 153, Feb. 2024.
- [19] X. Chen, Z. Zhang, Y. Zheng, Z. Chen, and C. Ruan, "Towards cis-lunar navigation: Design and analysis of a SmallSat system with time-transfer from BDS," in *Proc. China Satell. Navigat. Conf.*, 2024, pp. 438–448.
- [20] K. Wang, K. Li, S. Lv, Y. Jiao, Y. Shen, Z. Yue, and K. Xu, "Multi-orbit lunar GNSS constellation design with distant retrograde orbit and halo orbit combination," *Sci. Rep.*, vol. 13, no. 1, Jun. 2023, Art. no. 10158.
- [21] S. Kaplev, M. Titov, T. Valentirova, I. Mozharov, A. Bolkunov, and V. Yaremchuk, "Lunar PNT system concept and simulation results," *Open Astron.*, vol. 31, no. 1, pp. 110–117, Mar. 2022.
- [22] F. Pereira, P. M. Reed, and D. Selva, "Multi-objective design of a lunar GNSS," *J. Inst. Navigat.*, vol. 69, no. 1, Mar. 2022, Art. no. navi504.
- [23] K. Iiyama, S. Bhamidipati, and G. Gao, "Precise positioning and time-keeping in a lunar orbit via terrestrial GPS time-differenced carrier-phase measurements," *J. Inst. Navigat.*, vol. 71, no. 1, 2024, Art. no. nav1635.
- [24] Test Assessment Res. Center China Satell. Navigat. Office. *Constellation Status of Fundamental PNT Service China*. Accessed: Nov. 16, 2023. [Online]. Available: <http://www.csno-tarc.cn/system/constellation>
- [25] *Space Track*. Accessed: Nov. 18, 2023. [Online]. Available: <https://www.space-track.org/>
- [26] China Satell. Navigat. Office. (12, 2019). *The Application Service Architecture of BeiDou Navigation Satellite System (V1.0)*. [Online]. Available: <http://m.beidou.gov.cn/xt/gfzx/201912/P020191227333024390305.pdf>
- [27] M. Bolliger, M. R. Thompson, N. P. Re, C. Ott, D. C. Davis, and N. Parrish, "Ground-based navigation trades for operations in gateway's near rectilinear halo orbit," in *Proc. 31st AAS/AIAA Space Flight Mech. Meeting*, 2021, pp. 1–20.
- [28] China Satell. Navigat. Office. (2018). *BeiDou Navigation Satellite System Signal in Space Interface Control Document: Open Service Signal B3I (V1.0)*. [Online]. Available: <http://www.beidou.gov.cn/xt/gfzx/201802/P020180209623601401189.pdf>
- [29] E. E. Fowler, S. B. Hurtt, and D. A. Paley, "Orbit design for cislunar space domain awareness," in *Proc. 2nd IAA Conf. Space Situational Awareness*, 2020, pp. 1–12.
- [30] M. Hinga, "Cis-lunar autonomous navigation via implementation of optical asteroid angle-only measurements," in *Proc. 21st Adv. Maui Opt. Space Surveill. Technol. (AMOS) Conf.*, 2020, pp. 1–18.
- [31] J. Williams, D. E. Lee, R. J. Whitley, K. A. Bokelmann, D. C. Davis, and C. F. Berry, "Targeting cislunar near rectilinear halo orbits for human space exploration," in *Proc. 27th AAS/AIAA Space Flight Mech. Meeting*, 2017, pp. 1–20.
- [32] S. Trofimov, M. Shirobokov, A. Tselousova, and M. Ovchinnikov, "Transfers from near-rectilinear halo orbits to low-perilune orbits and the Moon's surface," *Acta Astronautica*, vol. 167, pp. 260–271, Feb. 2020.
- [33] R. J. Whitley, D. C. Davis, L. M. Burke, B. P. McCarthy, R. J. Power, M. L. McGuire, and K. C. Howell, "Earth-Moon near rectilinear halo and butterfly orbits for lunar surface exploration," in *Proc. AAS/AIAA Astrodynamics Spec. Conf.*, 2018, p. 264836399.
- [34] M. Schonfeldt, A. Grenier, A. Delépaut, P. Giordano, R. Swinden, J. Ventura-Traveset, D. Blonski, and J. Hahn, "A system study about a lunar navigation satellite transmitter system," in *Proc. Eur. Navigat. Conf. (ENC)*, Dresden, Germany, Nov. 2020, pp. 1–10.
- [35] P. Liu, X.-Y. Hou, J.-S. Tang, and L. Liu, "Application of two special orbits in the orbit determination of lunar satellites," *Res. Astron. Astrophys.*, vol. 14, no. 10, pp. 1307–1328, Oct. 2014.
- [36] Z.-Y. Gao and X.-Y. Hou, "Coverage analysis of lunar communication/navigation constellations based on halo orbits and distant retrograde orbits," *J. Navigat.*, vol. 73, no. 4, pp. 932–952, Jul. 2020.
- [37] M. A. Sirwah, D. Tarek, M. Radwan, and A. H. Ibrahim, "A study of the moderate altitude frozen orbits around the moon," *Results Phys.*, vol. 17, Jun. 2020, Art. no. 103148.
- [38] F. Pereira and D. Selva, "Exploring the design space of lunar GNSS in frozen orbit conditions," in *Proc. IEEE/ION Position, Location Navigat. Symp. (PLANS)*, Portland, OR, USA, Apr. 2020, pp. 444–451.
- [39] J. E. Donaldson, J. J. K. Parker, M. C. Moreau, D. E. Highsmith, and P. D. Martzen, "Characterization of on-orbit GPS transmit antenna patterns for space users," *Navigat.*, vol. 67, no. 2, pp. 411–438, Jun. 2020.
- [40] Y. Lv, T. Geng, Q. Zhao, X. Xie, and R. Zhou, "Initial assessment of BDS-3 preliminary system signal-in-space range error," *GPS Solutions*, vol. 24, no. 1, pp. 1–13, Jan. 2020.
- [41] Z. Ju, L. Chen, and J. Yan, "Acquisition of weak BDS signal in the lunar environment," *Remote Sens.*, vol. 15, no. 9, p. 2445, May 2023.



earth-moon space navigation and aerospace TT&C.

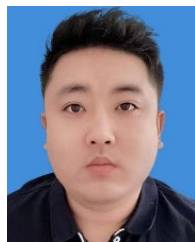
XIAO CHEN received the B.S. degree in environment simulation engineering and the M.S. degree in cartography and geographic information engineering from Information Engineering University, Zhengzhou, China, in 2009 and 2012, respectively, where he is currently pursuing the Ph.D. degree in surveying and mapping science and technology with the School of Geospatial Information. He is also an Aerospace Engineer with Xi'an Satellite Control Center. His research interests include



YONG ZHENG received the B.S. and M.S. degrees in geodesy from Zhengzhou Institute of Surveying and Mapping, Zhengzhou, China, in 1984 and 1989, respectively, and the Ph.D. degree in astrometry from Shanghai Astronomical Observatory, in 1992. He is currently a Professor with Information Engineering University. He is the author of more than 100 journal articles and has written three books. His current research interests include astrodynamics and celestial navigation.



LAN DU received the B.S. degree in space photography and the M.S. and Ph.D. degrees in geodesy and surveying engineering from Information Engineering University, Zhengzhou, China, in 1992, 1996, and 2006, respectively. She was a Visiting Scholar with German Research Centre for Geosciences (GFZ), Potsdam, Germany, in 2016. She is currently a Professor with Information Engineering University. Her research interests include astrodynamics, space geodesy, and orbit determination.



ZHONGKAI ZHANG received the B.S. degree in astronomy from Nanjing University, Nanjing, China, in 2011, the M.S. degree in astrometry and astrodynamics from Information Engineering University, Zhengzhou, China, in 2014, and the Ph.D. degree in geodesy and geoinformation from the University of Bonn, Bonn, Germany, in 2019. He was a Postdoctoral Researcher with Henan University, Zhengzhou, China, and a Visiting Scholar with the Max Planck Institute for Radio Astronomy, Bonn, Germany. He is currently an Associate Professor with Information Engineering University. His research interests include space geodesy, deep space exploration, and VLBI.